Обзор ArXiv/astro-ph, 31 сентября – 4 октября 2024

От Сильченко О.К.

NGC 5055 (SDSS) - Sbc

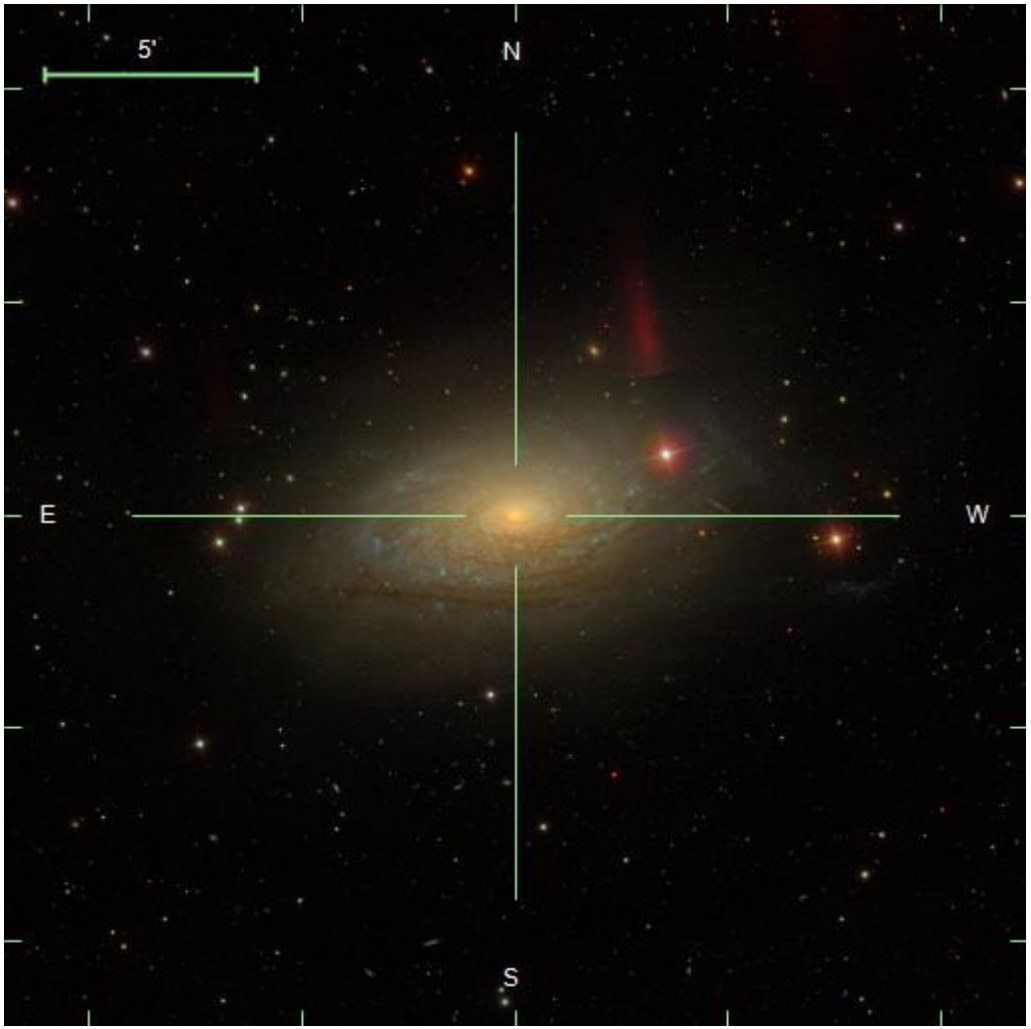

FAST: HI диск до >60 кпк от центра

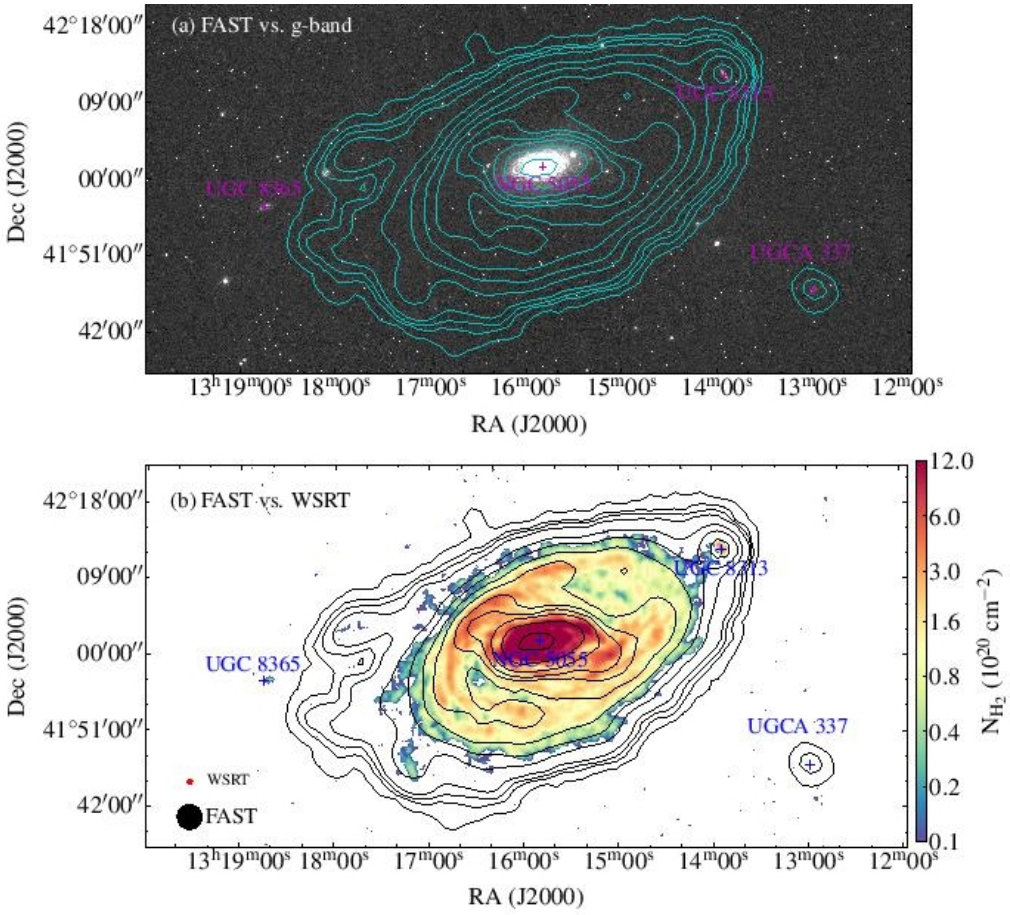

Fig. 1: H I column density contours in the velocity range of 276.0-718.8 km s^{-1} superimposed on the SDSS g-band optical image of the NGC 5055 galaxy group (a) and the HALOGAS survey data (b). The contours are 0.1 (3σ), 0.3, 0.6, 1.0, 3.3, 6.8, 12.8, 20.6, 31.4, 41.2, 55.5, 82.4, 123.4, 156.0$\times 10^{19}$ cm^{-2} respectively. The plus symbols indicate the optical centers of galaxies NGC 5055, UGC 8313, UGCA 337 and UGC 8365, respectively. The beamsizes of FAST and WSRT are shown in

Поле скоростей

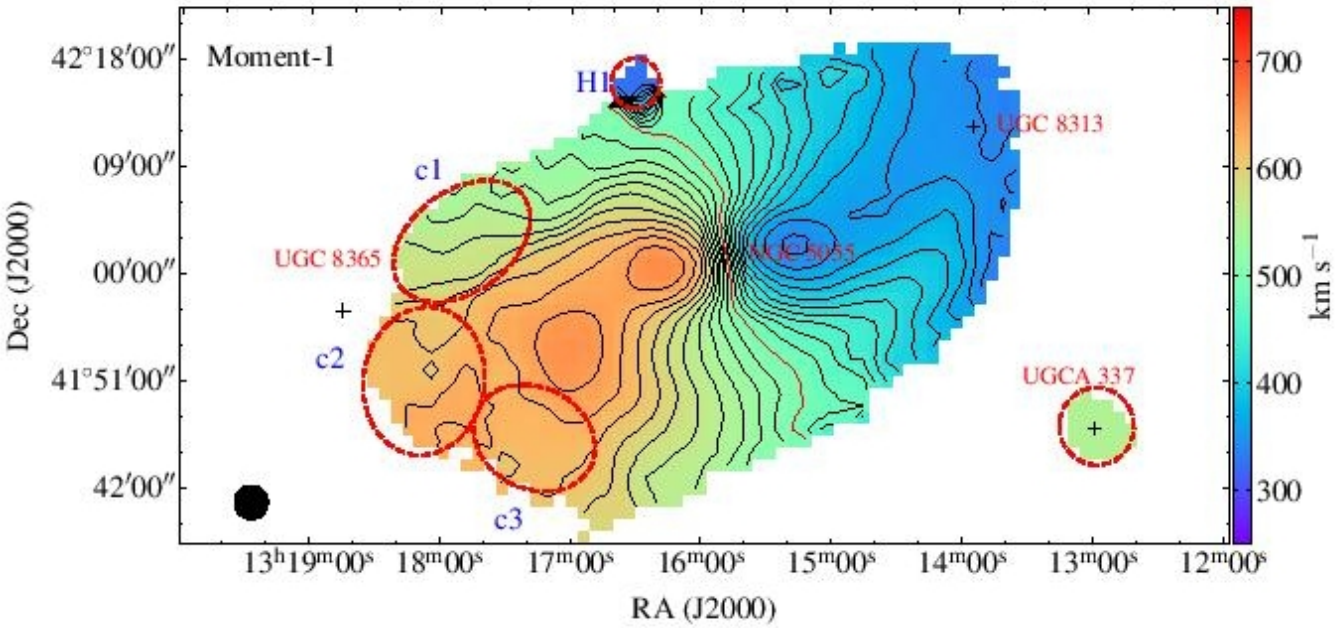

Fig. 4: H I intensity-weighted velocity field (i.e., the first moment map) of NGC 5055. UGC 8313 has been excluded in this calculation. Velocity contours start from 297.8 to 672.8 km s^{-1} in steps of 15 km s^{-1}. The red solid line denotes the system velocity of NGC 5055. Dashed ellipses/circles and pluses represent the same features as those in Figure 3. The beamsize of FAST is displayed in the bottom-left corner.

Облака HI без звезд

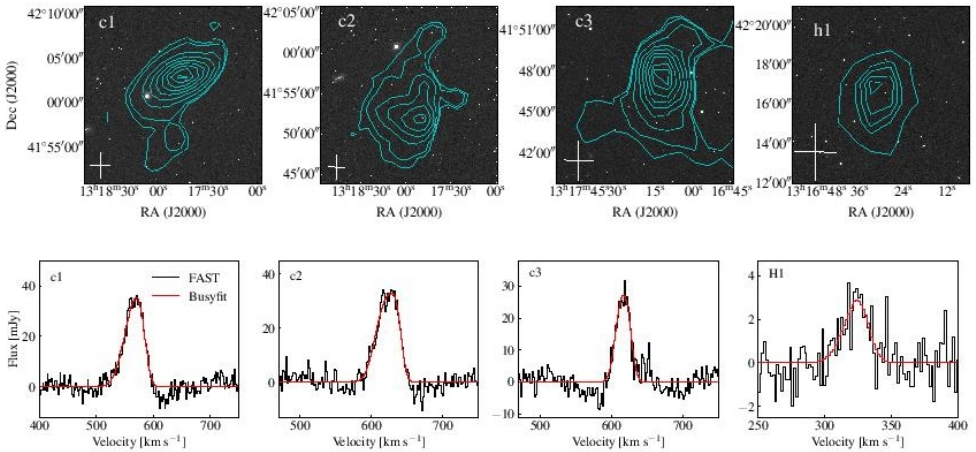

Fig. 5: Top: H I column density contours superimposed on the SDSS g-band optical image for clouds c1, 2, 3, along with the candidate HVC H1. Black contour levels for cloud c1 are 1.2 (3σ), 2.0, 4.5, 7.1, 9.7, 12.3, 14.8, 17.4, 20.0$\times10^{18}$ cm^{-2}, for cloud c2 are 1.2 (3σ), 2.0, 4.6, 7.1, 9.7, 12.3$\times10^{18}$ cm^{-2}, for cloud c3 are 2.0 (3σ), 5.0, 8.0, 10.9, 13.9, 16.9, 19.9, 22.0$\times10^{18}$ cm^{-2}, and for cloud H1 are 0.6 (3σ), 0.9, 1.0, 1.2, 1.3$\times10^{18}$ cm^{-2}. The beam size of FAST is displayed in the bottom-left corner in each panel. Bottom: The corresponding integrated H I spectra lines. The red lines represent the fittings from the busy function code (Westmeier

Table 1: The observed parameters for H I sources in the NGC 5055 galaxy group.

source	log(M$_{\rm H\,I}$) (M$_\odot$)	$S_{\rm H\,I}$ (mJy km s^{-1})	$S_{\rm peak}$ (mJy)	$v_{\rm sys}$ (km s^{-1})	W_{50} (km s^{-1})	W_{20} (km s^{-1})	Velocity range (km s^{-1})
(1)	(2)	(3)	(4)	(5)	(6)	(7)	(8)
FAST							
NGC 5055	10.03(0.01)	574.8(17.3) $\times$ 10^3	2390.0(131.2)	492.8(0.4)	346.7(0.5)	383.5(0.5)	276.0-718.8
UGCA 337	6.55(0.04)	194.7(17.5)	10.8(1.7)	550.0(1.0)	17.4(3.8)	25.3(5.6)	533.7-557.8
c1	7.43(0.01)	1449.0(43.2)	35.3(1.8)	564.5(0.8)	39.3(1.9)	58.2(2.5)	536.9-601.3
c2	7.36(0.01)	1239.0(36.2)	33.0(1.3)	621.6(0.6)	37.0(1.4)	51.1(1.9)	583.6-651.2
c3	7.09(0.02)	661.6(35.0)	27.2(2.5)	616.5(0.9)	23.6(2.9)	34.0(4.4)	590.0-657.7
H1	6.09(0.17)	66.0(25.5)	2.9(1.1)	322.8(3.7)	21.5(11.3)	33.0(17.0)	316.3-329.2
HALOGAS (after bp correction)							
NGC 5055	9.94(0.02)	469.6(19.8) $\times$ 10^3	1727.0(134.1)	497.9(0.6)	354.2(2.7)	389.1(1.9)	276.0-718.8

Спутник низкой поверхностной яркости, gas-poor

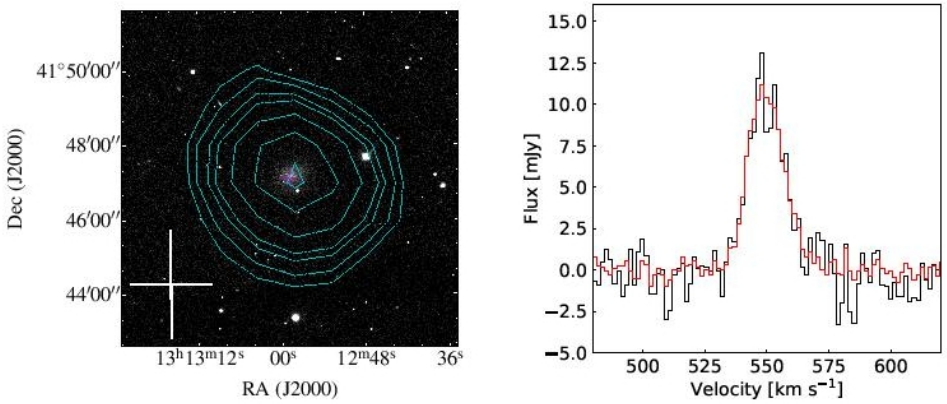

Fig. 6: Left: H I column density contours in the velocity range of 533.7-557.8 km s^{-1} superimposed on the SDSS g-band optical image for UGCA 337. The cyan contour levels are 1.0 (3σ), 1.4, 1.7, 2.4, 3.5 and 4.5×10^{18} cm^{-2}. The magenta plus marks the optical center of the galaxy. The beamsize of FAST is displayed in the bottom-left corner. Right: The corresponding integrated H I spectrum for UGCA 337. The red line represents the fitting from the busy function code (Westmeier et al. 2014).

Table 1: The observed parameters for H I sources in the NGC 5055 galaxy group.

source	$\log(M_{HI})$ ($M_\odot$)	S_{HI} (mJy km s^{-1})	S_{peak} (mJy)	v_{sys} (km s^{-1})	W_{50} (km s^{-1})	W_{20} (km s^{-1})	Velocity range (km s^{-1})
(1)	(2)	(3)	(4)	(5)	(6)	(7)	(8)
FAST							
NGC 5055	10.03(0.01)	$574.8(17.3)\times10^3$	2390.0(131.2)	492.8(0.4)	346.7(0.5)	383.5(0.5)	276.0-718.8
UGCA 337	6.55(0.04)	194.7(17.5)	10.8(1.7)	550.0(1.0)	17.4(3.8)	25.3(5.6)	533.7-557.8
c1	7.43(0.01)	1449.0(43.2)	35.3(1.8)	564.5(0.8)	39.3(1.9)	58.2(2.5)	536.9-601.3
c2	7.36(0.01)	1239.0(36.2)	33.0(1.3)	621.6(0.6)	37.0(1.4)	51.1(1.9)	583.6-651.2
c3	7.09(0.02)	661.6(35.0)	27.2(2.5)	616.5(0.9)	23.6(2.9)	34.0(4.4)	590.0-657.7
H1	6.09(0.17)	66.0(25.5)	2.9(1.1)	322.8(3.7)	21.5(11.3)	33.0(17.0)	316.3-329.2
HALOGAS (after bp correction)							
NGC 5055	9.94(0.02)	$469.6(19.8)\times10^3$	1727.0(134.1)	497.9(0.6)	354.2(2.7)	389.1(1.9)	276.0-718.8

ArXiv: 2409.20549

Detection of [OIII]$_{88\mu m}$ in JADES-GS-z14-0 at z=14.1793

Sander Schouws,[1] Rychard J. Bouwens,[1] Katherine Ormerod,[2] Renske Smit,[2] Hiddo Algera,[3,4] Laura Sommovigo,[5] Jacqueline Hodge,[1] Andrea Ferrara,[6] Pascal A. Oesch,[7,8,9] Lucie E. Rowland,[1] Ivana van Leeuwen,[1] Mauro Stefanon,[1] Thomas Herard-Demanche,[1] Yoshinobu Fudamoto,[10] Huub Röttgering,[1] and Paul van der Werf[1]

[1]*Leiden Observatory, Leiden University, NL-2300 RA Leiden, Netherlands*
[2]*Astrophysics Research Institute, Liverpool John Moores University, 146 Brownlow Hill, Liverpool L3 5RF, United Kingdom*
[3]*Hiroshima Astrophysical Science Center, Hiroshima University, 1-3-1 Kagamiyama, Higashi-Hiroshima, Hiroshima 739-8526, Japan*
[4]*National Astronomical Observatory of Japan, 2-21-1, Osawa, Mitaka, Tokyo, Japan*
[5]*Center for Computational Astrophysics, Flatiron Institute, 162 Fifth Avenue, New York, NY 10010, USA*
[6]*Scuola Normale Superiore, Piazza dei Cavalieri 7, 50126 Pisa, Italy*
[7]*Departement d'Astronomie, Université de Genéeve, 51 Ch. des Maillettes, CH-1290 Versoix, Switzerland*
[8]*Cosmic Dawn Center (DAWN), Copenhagen, Denmark*
[9]*Niels Bohr Institute, University of Copenhagen, Jagtvej 128, DK-2200 Copenhagen N, Denmark*
[10]*Center for Frontier Science, Chiba University, 1-33 Yayoi-cho, Inage-ku, Chiba 263-8522, Japan*

ABSTRACT

We report the first successful ALMA follow-up observations of a secure $z > 10$ JWST-selected galaxy, by robustly detecting (6.6σ) the [OIII]$_{88\mu m}$ line in JADES-GS-z14-0 (hereafter GS-z14). The ALMA detection yields a spectroscopic redshift of $z = 14.1793 \pm 0.0007$, and increases the precision on the prior redshift measurement of $z = 14.32^{+0.08}_{-0.20}$ from NIRSpec by $\gtrsim$180×. Moreover, the redshift is consistent with that previously determined from a tentative detection (3.6σ) of CIII]$_{1907,1909}$ ($z = 14.178 \pm 0.013$), solidifying the redshift determination via multiple line detections. We measure a line luminosity of $L_{[OIII]88} = (2.1 \pm 0.5) \times 10^8\, L_\odot$, placing GS-z14 at the lower end, but within the scatter of, the local $L_{[OIII]88}$-star formation rate relation. No dust continuum from GS-z14 is detected, suggesting an upper limit on the dust-to-stellar mass ratio of $< 2 \times 10^{-3}$, consistent with dust production from supernovae with a yield $y_d < 0.3\, M_\odot$. Combining a previous JWST/MIRI photometric measurement of the [OIII]$\lambda\lambda$4959,5007Å and Hβ lines with Cloudy models, we find GS-z14 to be surprisingly metal-enriched ($Z \sim 0.05 - 0.2\, Z_\odot$) a mere 300 Myr after the Big Bang. The detection of a bright

Характеристики самой далекой галактики

Table 1. Properties of GS-z14

Parameter	**Value**
RA	03:32:19.9049
Dec	−27:51:20.265
Redshift	$z = 14.1793(7)$
M_{UV}	-20.81 ± 0.16
Stellar Mass ($\log(M_\odot)$)	$8.7^{+0.5}_{-0.4}$
Star Formation Rate ($M_\odot$/yr)	25^{+6}_{-5}
$[OIII]_{88\mu m}$ Luminosity ($10^8\,L_\odot$)	2.1±0.5
FWHM $[OIII]_{88\mu m}$ (km s^{-1})	136±31
Dynamical Mass ($M_\odot$ $(\sin i)^2$)	$(1.0\pm0.5)\times10^9$
90-μm continuum flux (μJy/beam)	< 15.1 (3σ)
Dust Mass ($\log(M_\odot)$)	< 6.0

Notes: M_{UV} from Carniani et al. (2024); stellar mass and SFR from Helton et al. (2024). Values have been corrected for a lensing magnification of 1.17× (Carniani et al. 2024).

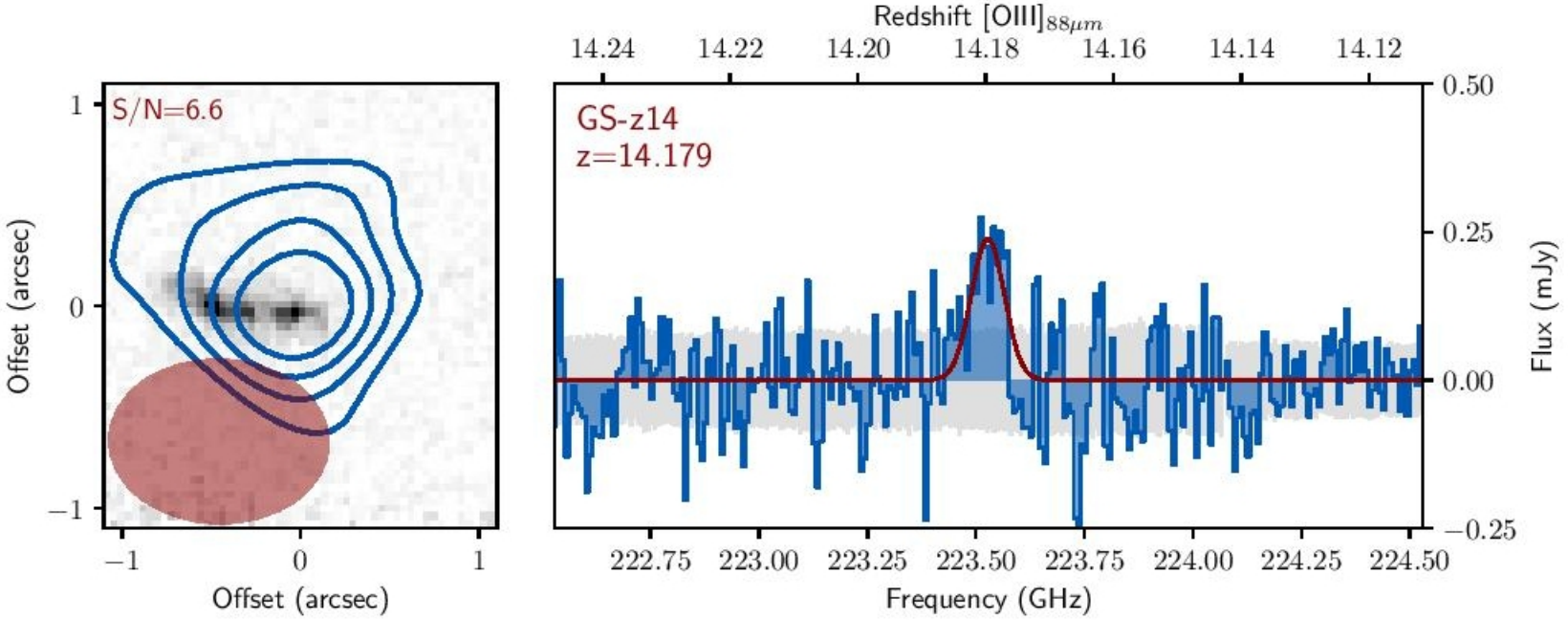

Figure 2. Detection of [OIII]$_{88\mu m}$ in GS-z14 at $z = 14.1793 \pm 0.0007$. *Left Panel:* Contours showing the [OIII]$_{88\mu m}$ emission (2, 3, 4 and 5σ) overlaid on the F200W imaging (Eisenstein et al. 2023a,b). The [OIII]$_{88\mu m}$ emission is detected at a peak significance of 6.6σ in the collapsed data-cube. *Right Panel:* The spectrum of the [OIII]$_{88\mu m}$ line (*blue histogram*) extracted from the >3σ emission region in the moment-0 map. The red line shows the Gaussian fit used to measure the spectroscopic redshift and FWHM of the line. The grey shaded region indicates the 1σ uncertainties.

ArXiv: 2409.20533

The eventful life of a luminous galaxy at $z = 14$: metal enrichment, feedback, and low gas fraction?

Stefano Carniani[1], Francesco D'Eugenio[2,3,4], Xihan Ji[2,3], Eleonora Parlanti[1], Jan Scholtz[2,3], Fengwu Sun[5], Giacomo Venturi[1], Tom J. L. C. Bakx[6], Mirko Curti[7], Roberto Maiolino[2,3,8], Sandro Tacchella[2,3], Jorge A. Zavala[9], Kevin Hainline[10], Joris Witstok[11,3], Benjamin D. Johnson[5], Stacey Alberts[10], Andrew J. Bunker[12], Stéphane Charlot[13], Daniel J. Eisenstein[5], Jakob M. Helton[10], Peter Jakobsen[11,14], Nimisha Kumari[15], Brant Robertson[16], Aayush Saxena[12,8], Hannah Übler[2,3], Christina C. Williams[17], Christopher N. A. Willmer[10], and Chris Willott[18]

[1] Scuola Normale Superiore, Piazza dei Cavalieri 7, I-56126 Pisa, Italy
[2] Kavli Institute for Cosmology, University of Cambridge, Madingley Road, Cambridge, CB3 0HA, UK
[3] Cavendish Laboratory, University of Cambridge, 19 JJ Thomson Avenue, Cambridge, CB3 0HE, UK
[4] INAF – Osservatorio Astronomico di Brera, via Brera 28, I-20121 Milano, Italy
[5] Center for Astrophysics | Harvard & Smithsonian, 60 Garden St., Cambridge MA 02138 USA
[6] Department of Space, Earth, & Environment, Chalmers University of Technology, Chalmersplatsen 4 412 96 Gothenburg, Sweden
[7] European Southern Observatory, Karl-Schwarzschild-Strasse 2, 85748 Garching, Germany
[8] Department of Physics and Astronomy, University College London, Gower Street, London WC1E 6BT, UK
[9] National Astronomical Observatory of Japan, 2 Chome-21-1, Osawa, Mitaka, Tokyo 181-8588, Japan
[10] Steward Observatory, University of Arizona, 933 N. Cherry Avenue, Tucson, AZ 85721, USA
[11] Cosmic Dawn Center (DAWN), Copenhagen, Denmark
[12] Department of Physics, University of Oxford, Denys Wilkinson Building, Keble Road, Oxford OX1 3RH, UK
[13] Sorbonne Université, CNRS, UMR 7095, Institut d'Astrophysique de Paris, 98 bis bd Arago, 75014 Paris, France
[14] Niels Bohr Institute, University of Copenhagen, Jagtvej 128, DK-2200, Copenhagen, Denmark
[15] AURA for European Space Agency, Space Telescope Science Institute, 3700 San Martin Drive. Baltimore, MD, 21210
[16] Department of Astronomy and Astrophysics University of California, Santa Cruz, 1156 High Street, Santa Cruz CA 96054, USA
[17] NSF's National Optical-Infrared Astronomy Research Laboratory, 950 North Cherry Avenue, Tucson, AZ 85719, USA
[18] NRC Herzberg, 5071 West Saanich Rd, Victoria, BC V9E 2E7, Canada

Prospector: подгонка SED

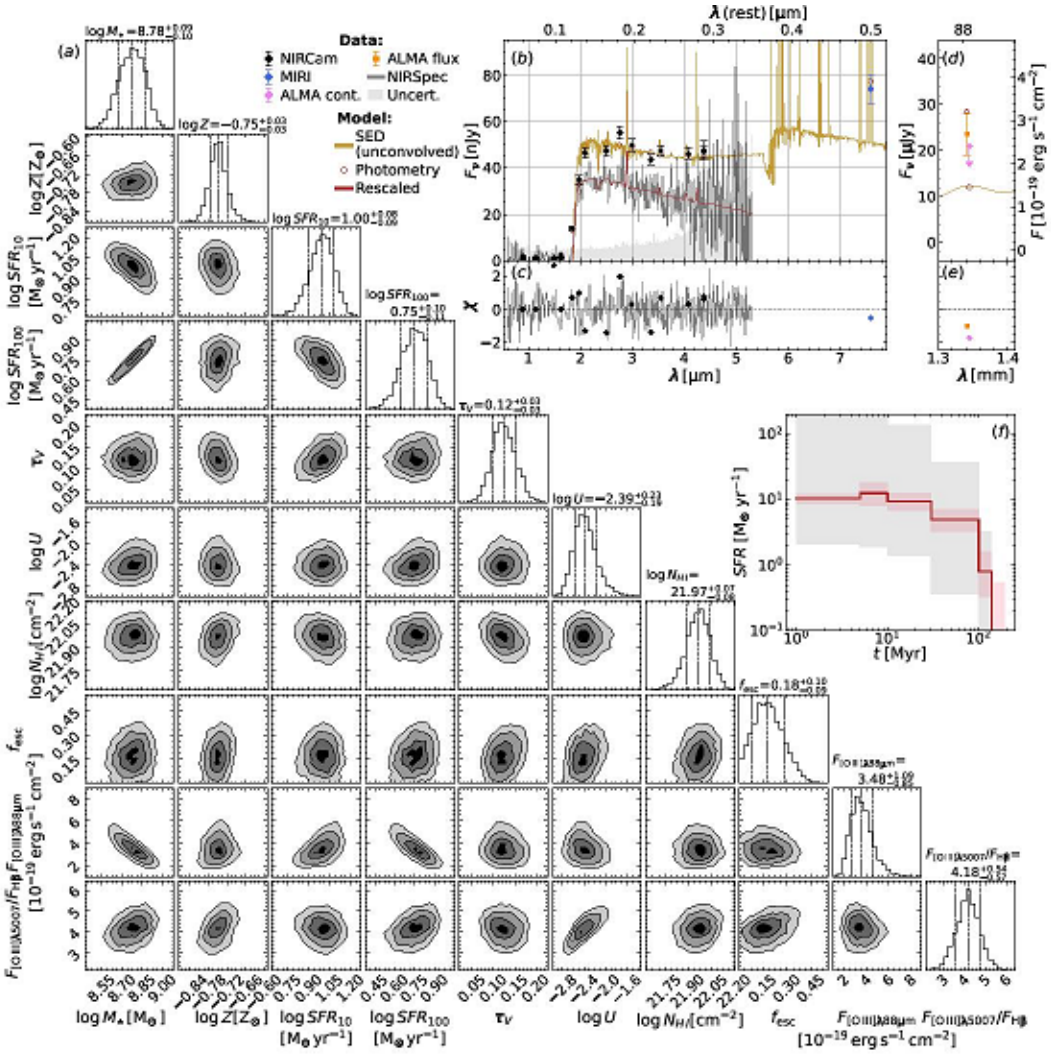

Fig. 5: Summary of `prospector` SED model. Panel a. Triangle diagram with the marginalised posterior distribution over a subset of the model-free or dependent parameters (see Table 2 for a description of the parameters and their probability prior). Panel b. SED, including wide- and medium-band measured flux densities (diamonds), the spectrum (grey line with grey region as the uncertainty). NIRCam, MIRI and ALMA data are in black, blue and pink, respectively. Model predictions are red circles (flux densities) or the red line (spectrum). The sand-coloured line is the model SED without convolving to the spectral resolution fo the data. Panel c. Model residuals normalised by the uncertainties. Panel d. Same as panel b, but for the FIR region. The orange square is the ALMA [O III] flux. Panel e. Same as panel c, but for the FIR region. Panel f. Star-formation history (red), with the prior probability in grey.

Умеренное звездообразование

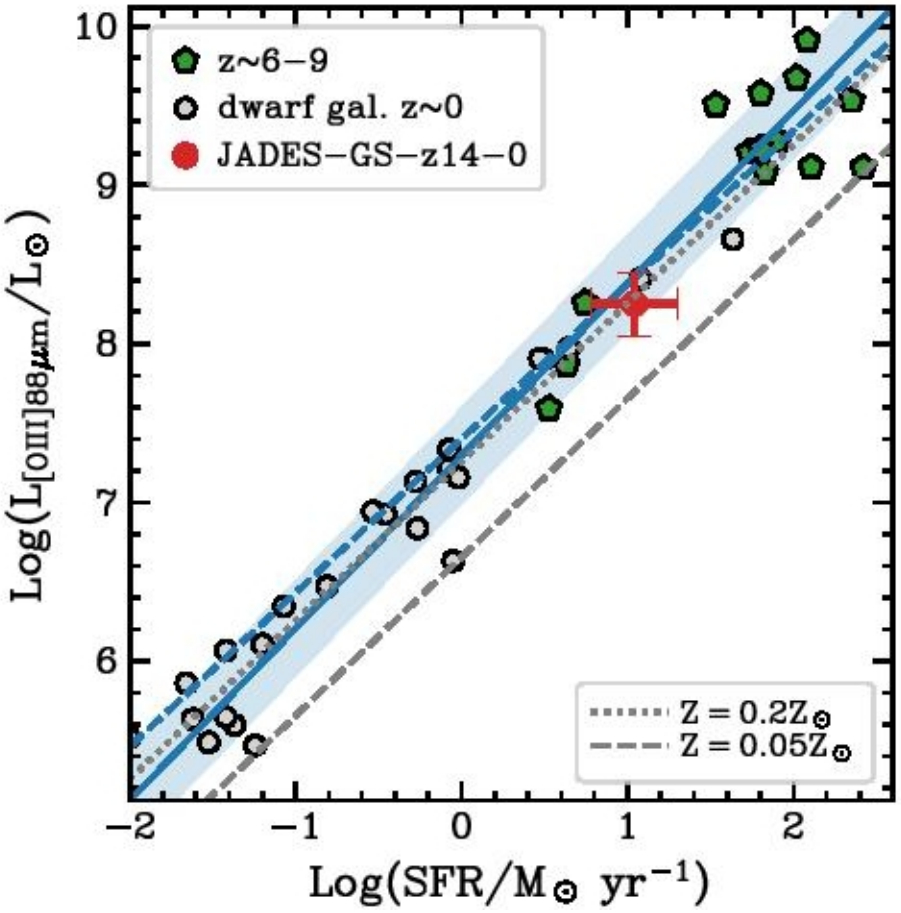

Умеренная химия

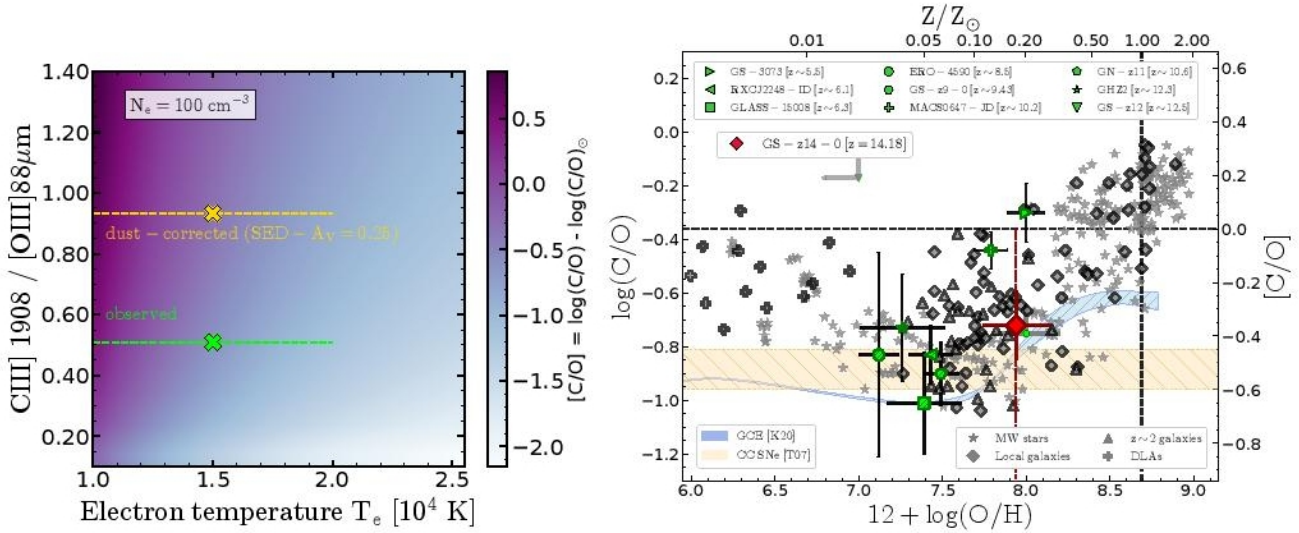

Fig. 6: Carbon-over-oxygen abundance for JADES-GS-z14-0. The left-hand panel shows how the final inferred C/O value changes as a function of the C III]/[O III] 88μm line ratio and of the electron temperature, T_e, under our fiducial assumption of N_e=100 cm^{-3}. The observed and dust-corrected C III]/[O III] 88μm ratios for JADES-GS-z14-0 are marked in green and yellow, respectively. In the right-hand panel, we report our fiducial C/O measurement for JADES-GS-z14-0 on the C/O vs O/H diagram. The oxygen abundance is inferred from the best-fit PROSPECTOR metallicity reported in Table 2. The C/O value measured in JADES-GS-z14-0 is consistent with pure enrichment from core-collapse Supernovae. We also report for comparison a sample of C/O measurements from JWST compiled from the literature, namely GS-z12 (z = 12.5; D'Eugenio et al. 2024b), GHZ2 (z = 12.34; Castellano et al. 2024), GN-z11 (z = 10.6; Cameron et al. 2023), MACS0647-JD (z = 10.2; Hsiao et al. 2024), GS-z9-0 (z = 9.4; Curti et al. 2024), ERO-4590 (z = 8.5; Arellano-Córdova et al. 2022), RXCJ2248-ID (z = 6.11; Topping et al. 2024), GLASS-150008 (z = 6.23; Jones et al. 2023), GS-3073 (z=5.5; Ji et al. 2024). The C/O vs O/H pattern predicted by Galactic Chemical Evolution models of Kobayashi et al. (2020) is shown in blue, whereas the C/O range allowed by the CC-SNe yields from Tominaga et al. (2007) is marked by the golden region.